ISSN 1063-7796, Physics of Particles and Nuclei, 2022, Vol. 53, No. 1, pp. 59–77. © Pleiades Publishing, Ltd., 2022.
Russian Text © The Author(s), 2022, published in Fizika Elementarnykh Chastits i Atomnogo Yadra, 2022, Vol. 53, No. 1.

The Phenomenon of Artificial Radioactivity in Metal Cathodes under Glow Discharge Conditions

S. F. Timashev[a], I. B. Savvatimova[a], S. S. Poteshin[a], N. I. Kargin[a], A. A. Sysoev[a], and S. M. Ryndya[a, *]

[a] *National Research Nuclear University MEPhI, Moscow, 115409 Russia*

**e-mail: SMRyndya@mephi.ru*

Received April 30, 2021; revised June 15, 2021; accepted July 12, 2021

Abstract—It is shown that artificial radioactivity can be initiated under conditions of a glow-discharge plasma. When analyzing the isotopic and elemental composition in the near-surface region of Pd and Ni cathodes, initial and those treated for 40 hours under conditions of deuterium- or protium-containing plasma, changes were detected, respectively, in the isotopic ratios of Pt and Pb impurity isotopes in the Pd cathode and of Fe, Cu, and Zn in the Ni cathode, as well as a significant reduction in the amount of these impurity elements in the cathodes and the formation of W isotopes in the Pd cathode. Possible nuclear processes that cause the established artificial radioactivity are considered.

DOI: 10.1134/S1063779622010051

1. INTRODUCTION

The phenomenon of low-energy nuclear reactions (LENR) has been discussed most acutely in the last 30 years after the publication of the work of Fleishmann, Pons, and Hawkins [1], in which, in the electrolysis of heavy water D_2O with a Pd cathode, the formation of neutrons and tritium with a simultaneous excessive release of heat was detected. This result could not be understood within the well-known concepts of nuclear physics, according to which such processes could be produced only by the fusion of deuterium nuclei, which requires energies higher by at least six orders of magnitude and had to be accompanied by hazardous radiation, which, under the conditions of the experiment in [1], were not detected. Therefore, the physical community could not accept this result.

It should be pointed out that, historically, the first work in this direction, which was defined as "cold nuclear fusion" and somewhat later as "low-energy nuclear reactions," was the study of Wendt and Irion [2], who observed the appearance of helium atomic lines during the explosion of a tungsten wire in a glass flask, inside which a vacuum was created. Rutherford in his short note [3] explained that the formation of helium under such conditions is impossible, since the kinetic energy of electrons during the explosion of a tungsten wire was only about 6 eV. At the same time, as shown by special experiments carried out in Rutherford's laboratory, no formation of helium was observed even in X-ray tubes with long-term irradiation of tungsten targets by electrons with a kinetic energy of about 100 keV. Nevertheless, Wendt [4] disagreed with Rutherford, pointing out that the power released in the explosion of a tungsten wire is many orders of magnitude higher than the power absorbed by a target in an X-ray tube, where the current is of milliamperes or less, and that it is high particle-collision velocities under explosion conditions that can lead to fission of tungsten nuclei. Naturally, the scientific community took the side of Rutherford, and article [2], in fact, was recognized as erroneous.

We should note here a few more subsequent studies in which the formation of products of nuclear transformations at relatively low energies was detected. First of all, these are the studies of the early 1950s by the group of Artsimovich of powerful electric discharges in tubes containing mixtures of deuterium and inert gases [5, 6]. It was found that, at partial pressures of deuterium up to several tens of Torr and applied voltages of several tens of kV, short pulses of neutrons and hard X-ray quanta with energies of ~300–400 keV were simultaneously generated in the middle region of the discharge tubes. A neutron radiation intensity of 10^8 neutrons per pulse at a current of 200 kA was detected. Moreover, at the moment when quanta with such a high energy appeared, the voltage applied to the discharge tube was only about 10 kV. The neutron indicator in these experiments was the induced radioactivity of a silver target placed in a paraffin block near the discharge tube, and the neutron flux was calculated based on the data on the formation of radioactive isotopes ^{108}Ag and ^{110}Ag in the target. In [5, 6], the question of the formation of neutrons and quanta of the indicated energies under the conditions of the

experiment in question remained open. The authors of [5, 6] excluded the possibility of the thermonuclear process $d + d \rightarrow {}^3\mathrm{He} + n$ under conditions of a low-temperature plasma. It should be noted that, although subsequent theoretical estimates [7–9] showed the theoretical possibility of such processes due to the deuteron-accelerating induced electric field during the development of instabilities in the pinch, doubts about the realization of the aforementioned thermonuclear reaction in the experiments [5, 6] remain: in these experiments, no helium-3 was detected, the amount of which in the discharge tube in this reaction should correspond to the total number of emitted neutrons.

A study with similar results was carried out by Basov and his team [10]. It was shown that, upon focusing short ($\sim 10^{-11}$ s) optical pulses of a powerful neodymium laser (irradiation intensity of $J_e \approx 10^{16}$ W/cm^2) on the surface of a LiD target, resulting in the formation of a nonstationary low-temperature plasma, in the volume of this plasma, neutrons were generated synchronously with the pulses. According to the estimates made in [10], under these actions, one neutron (on average) per laser pulse was detected. As shown in the recent work [11], the neutrons detected in [10] could be generated only in low-energy nuclear processes. This conclusion is consistent with the known data [12, 13] according to which direct initiation of nuclear processes is possible when using picosecond laser pulses with a peak intensity $J_e \sim (10^{18}–10^{19})$ W/cm^2. In particular, in these cases, the rate of spontaneous decays of nuclides can be increased by orders of magnitude.

The phenomenon of low-energy nuclear transformations was actually investigated also in the works of Deryagin and his team, conducted since the 1950s [14, 15], when the emission of high-energy (up to 100–150 keV) electrons from the surfaces of solids was detected after the separation of polymer films from them in a high vacuum and the formation of microcracks in the surface layer of solids. To determine the energy of electrons emitted by the newly formed surfaces of the crack walls, the X-ray characteristics of the crack zone were analyzed and the formation of the plasma state of the material in the propagating crack was established. The final stage of these studies was the discovery by Deryagin together with Klyuev, Lipson, and Toporov in 1986 of neutron generation [16, 17] during the destruction of D_2O ice targets by a metal bullet moving with an initial speed of 100–200 m/s. In this case, the number of generated neutrons was several times greater than the background level. In the case of a similar action on ordinary ice (H_2O), no neutron generation was detected.

Despite these publications, wide interest in the LENR phenomenon appeared only after the results of [1] had become known. However, soon after the publication of the results, it became clear, and this opinion persists to this day, that, within the concepts existing in nuclear physics, it is impossible to understand the very phenomenon of the initiation of nuclear processes at low energies and the almost complete absence of hazardous radiation accompanying nuclear reactions. At the same time, over the 30 years that have passed since the publication of [1], a wide diversity of new data has been obtained and presented in publications of leading scientific journals (see, e.g., [11, 18–21]) and at numerous international conferences (e.g., [22–24]).

Based on the analysis of the available literature, we believe that the key problem of finding out the mysterious essence of the LENR phenomenon comes down to an adequate understanding of the dynamics of nuclear transformations during the interaction of components of a nonequilibrium low-temperature plasma, which, explicitly or implicitly, is almost always manifested in the LENR processes, with metal surfaces. Therefore, of most interest from the viewpoint of understanding the physical essence of the LENR phenomenon may be the studies of such processes under conditions of a low-temperature plasma formed during a glow discharge in protium- and deuterium-containing gaseous media [25–27], as well as during laser ablation of metals in aqueous media [28–32].

It may be assumed that, when initiating nuclear processes under such conditions with mass spectrometric monitoring of the isotopic composition of the initial materials and products formed after appropriate treatment in a low-temperature plasma, it becomes possible to reveal the nature of the changes occurring in the isotopic and elemental (chemical) composition of the initial components.

It is on the basis of such general guidelines that this article is built, which presents the results of studying the effects of low-temperature nonequilibrium plasma of a glow discharge in protium- and deuterium-containing gas media on palladium and nickel cathodes, respectively, and uses the mass spectrometric analysis of the composition of the cathodes, original and plasma treated. In order to analyze the changes in the relative content of palladium and nickel isotopes as the main elements of the cathodes under study and detected impurity elements contained in the cathodes, as well as changes in the quantitative content of impurity elements, we used the ideas previously developed by one of us about the possibility of formation in a low-temperature plasma—in the vicinity of the cathode emitting nonequilibrium electrons—of metastable neutral nuclei with a locally disturbed ("β nuclei") nuclear structure [33–37]. Such β nuclei can be formed (see Section 3) upon inelastic scattering of high-energy (on the "chemical" scales) electrons with kinetic energies $E_e \sim (3–5)$ eV through the weak interaction between the nuclei of ions and atoms of the initial gaseous medium and metals knocked out from the

near-surface regions of the cathodes during plasma treatment. It should be emphasized here that, in the considered versions of low-temperature nonequilibrium plasma, the energy of electrons in the near-cathode region is on this scale. This is extremely important, since, at high kinetic energies (~10 eV and more), the energy of electrons will be mainly spent on the ionization of atoms and ions in the resulting nonequilibrium plasma. It should also be noted that, in [33–37], there are sufficiently many examples showing how neutron-like β nuclei can act as initiators of various nuclear processes. This is why we expressed the hope of using this basis for understanding the LENR phenomenon.

In this case, special attention will be paid to the analysis of the experimentally detected reduction in the initial content of impurity nonradioactive elements in both cathode materials: palladium and nickel.

2. EXPERIMENTAL

2.1. Experimental Setup and Sample Preparation

The glow-discharge setup in which a nonequilibrium protium- and/or deuterium-containing low-temperature plasma was produced included a vacuum chamber with a volume of 2×10^{-3} m^3 with a body in the form of a double quartz glass tube with spacing between the outer and inner tubes and bounded by flanges cooled by running water and electrode holders from Cr18Ni10Ti stainless steel, a vacuum system, a gas supply system, a cooling system, a custom-made pulse power supply, and a Tektronix TDS 3034C oscilloscope. The applied current I was from 10 to 300 mA, and the applied voltages were from 10 to 50 V. The magnitudes of the pulsed current and voltage recorded in the experiments by the Tektronix oscilloscope were $I \approx (1–6)$ A and $U \approx (1–8)$ kV, respectively, and the frequency f of the recorded current varied from 50 kHz to 50 MHz. Figures 1 and 2a show a photograph and a schematic diagram of the glow discharge setup, and Fig. 2b shows the placement of a sample in the glow discharge chamber.

The end parts of the anode and cathode, which contact the discharge plasma, were made of pure molybdenum produced by vacuum melting. The exposure time of the samples varied from several hours to tens of hours (from 7 to 40 h). The palladium and nickel samples with a thickness of about 100 μm and a diameter of 20 mm were placed on the cathode surface and fixed with squeezing restrainers made of molybdenum. The irradiation area was about 1 cm^2. After evacuation, the discharge chamber was filled with a plasma-forming gas to a pressure of 5–10 Torr. In the experiments with palladium, the plasma-forming gas was deuterium and, in the experiments with nickel, protium.

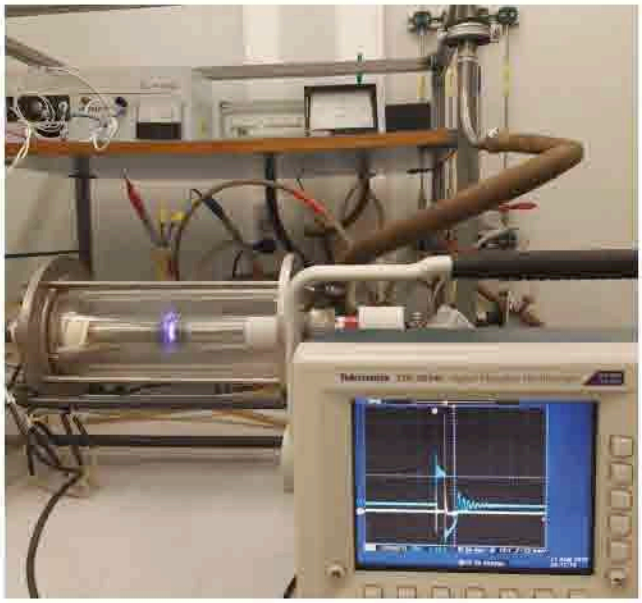

Fig. 1. Glow-discharge setup (the sample is the light spot on the left electrode holder; $I_{max} = 1.1$ A and $U_{max} = 5.3$ kV).

Figure 3 shows a typical "stable" pulsed discharge in a deuterium medium at $I_{max} = 1.3$ A (*1*), $U_{max} = 2.5$ kV (*2*), and $f = 6.2$ MHz.

Depending on the parameters of the discharge, plasma-forming gas, and irradiated material, the plasma discharge is not always stable. The photos presented in Figs. 4 and 5 show the regions of a Pd-D discharge with the highest intensity, which are visible as brighter spots on the irradiated sample, and "rays" with a higher luminosity and even with visible discrete regions with higher density in the lower plasma ray in the discharge gap.

A discharge in a hydrogen medium with a nickel sample has different parameters and is somewhat more stable. Instability in this case looks somewhat different (Fig. 6). The amplitude of the pulse current increases by a factor of seven (Fig. 6b).

2.2. Mass Spectrometric Elemental and Isotopic Analysis of Samples

The mass spectrometric analysis of the composition of the surface layers of the Pd and Ni cathodes, both initial and after plasma treatment, was performed using an ELAN DRC-e ICP (PerkinElmer, Canada) mass spectrometer for isotope and elemental analysis with an UP-213 laser ablation device (New Wave Research, United States). Inductively coupled plasma mass spectrometry (ICP-MS) is recognized as the most versatile method for analyzing the elemental and isotopic composition of a substance and is used as a fast, efficient, and highly sensitive method for the

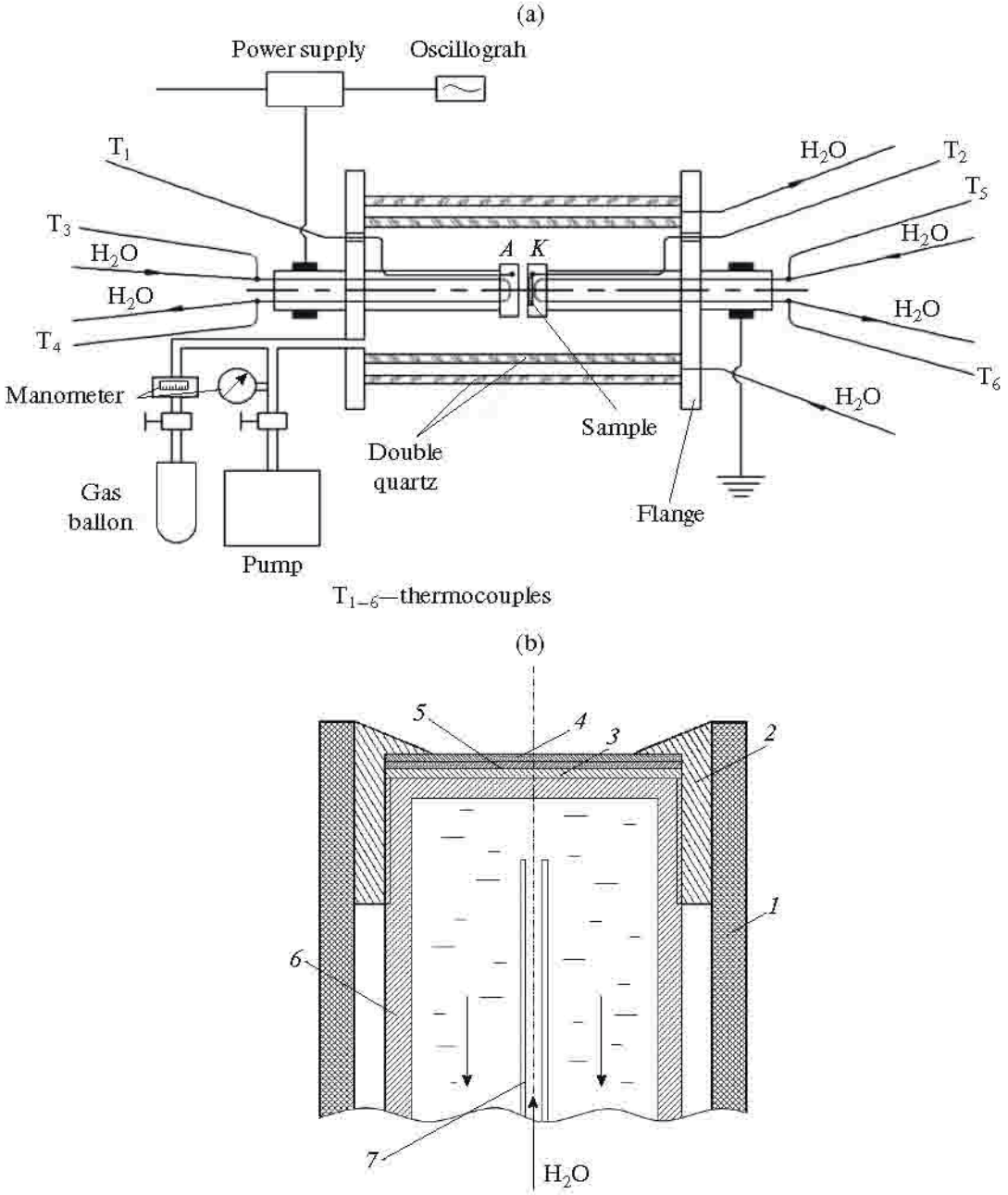

Fig. 2. (a) Schematic layout of the glow-discharge setup. (b) Layout of the sample in the glow discharge chamber: (*1*) quartz tube, (*2*) sample holder made of high purity vacuum-melted Mo, variant I: (*3*) W substrate with a thickness of 100 μm, (*4*) and (*5*) Pd), variant II: (*3*) and (*5*) Mo, (*4*) Ni foil with a thickness of 100 μm, (*6*) cooled electrode holder made of Cr18Ni10Ti steel, (*7*) tube made of Cr18Ni10Ti steel, supplying cooling water.

simultaneous quantitative determination of many elements in a wide concentration range. During laser scanning of a selected area of the sample surface and material ablation, a plasma is formed containing aerosol particles with sputtered metal components, which are captured by an argon flow and directed to the ICP burner. The plasma temperature is 6000–8000°C. There, a controlled ionization of the sample takes place, and then the free ions of the sample are separated according to the ratio mass-to-charge ratio $m_i/Z_i e$, where Z_i is the degree of ionization, e is the elementary charge, and m_i is the mass of ion i, and they are detected. In this case, a dual-mode (counting and analog) detector is used with an automatic selection of the operating mode with an operating linear range of more than nine orders of magnitude. In fact, at the exit, tables presenting the number of pulses per second are produced. They use "mass numbers," the m_i/Z_i

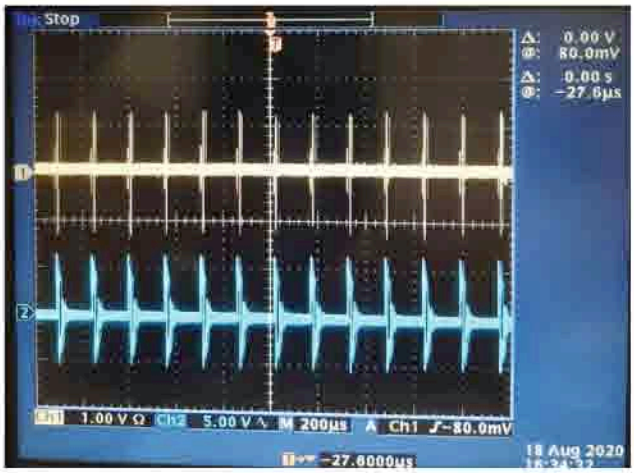

Fig. 3. Typical "stable" pulse discharge in a deuterium medium; (*1*) I_{max} = 1.3 A, (*2*) U_{max} = 2.5 kV, and f = 6.2 MHz.

ratios for each of the determined (according to a given program) ratios. The problems arising in the cases of $Z_i \neq 1$ are solved in each case separately. The range of analyzed masses is 5–260 amu, the resolution is 0.3–0.7 amu (in the range 5–260 amu), and the measurement accuracy of isotopic ratios is 0.08%. The scanning area is 6 × 2 mm^2 for the Pd sample and 3 × 1 mm^2 for the Ni sample. The size of the focused spot on the sample during ablation was ~80 μm, and the power density in the pulse was ~1–3 × 10^9 W/cm^2.

During the interaction of the focused high-power laser radiation with the surface, a strong instantaneous heating of the local area occurs, which leads to an explosive thermal evaporation of the sample components. In such evaporation regimes, the effects of mass discrimination of isotopes can be manifested at the sampling stage, but, in practice, they are noticeably manifested for light elements, usually with masses lower than 30 amu. For the selected range of mass numbers ~100–220 for the Pd sample and in the range ~50–70 for the Ni sample, the mass fractioning effects in the samples should be small. Nevertheless, to reduce the possible isotope fractionation effect, we used up to 15 samples sequentially obtained by ablation from each selected area. In this case, the background (without ablation) was measured, which was subtracted in the analysis. The number of measured pulses corresponding to the mass related to the ith isotope of element q are summed over all 15 successive measurements of the samples, and, then, these total values N_{qi} are analyzed as quantitative characteristics of the total number of this isotope of each specific element entering into the sample. In this case, it is actually assumed that the true number of each isotope in the sample mass is $N_{qi}^{tot} = A^{tot} N_{qi}$, where A^{tot} is a quantity that is constant for the specified conditions of the analysis. Since, under the conditions of any experiment, it is difficult to exclude uncontrollable factors, especially if the experiment is carried out at different times, the value of A^{tot} may vary.

It should be borne in mind here that the number of recorded pulses was largely determined by multiple defects in the structure of the surface layers of the samples. Naturally, for samples that had undergone a sufficiently long (for 40 hours) treatment in a glow discharge plasma, the defectiveness of the structure increased to a greater extent due to the long action of plasma flows on the samples, manifesting itself in changes in the morphology of the sample surface with the formation of inhomogeneities of the macro- and microrelief [38]. It is obvious that an increase in the defectiveness of the structure leads to a greater tendency of the metal to destruction, which manifests itself in an increase by an order of magnitude or more in the number of detected pulses corresponding to the basic elements of the cathodes when testing the sample after treatment in a glow discharge.

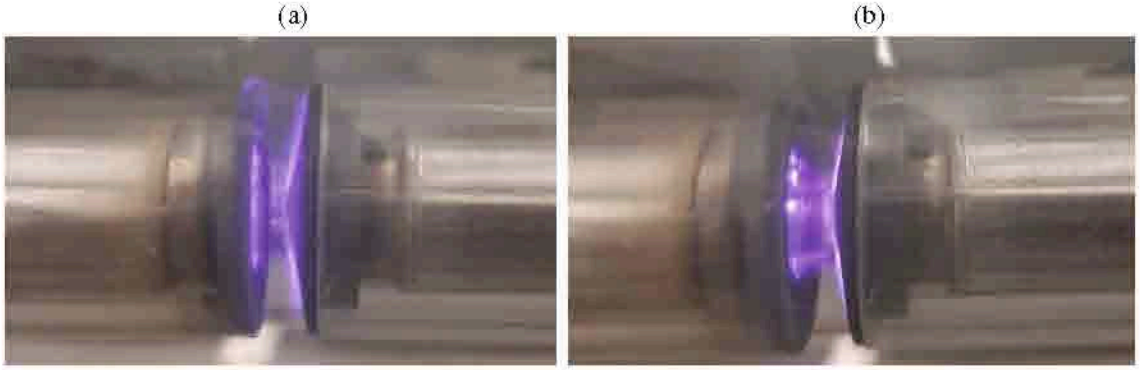

Fig. 4. Zone of the discharge gap in a deuterium medium on a palladium sample: (a) "stable" discharge; (b) "unstable" discharge; one can see brighter spots on the palladium sample (left) and brighter "rays" in the discharge gap and discrete denser regions in the lower plasma "ray."

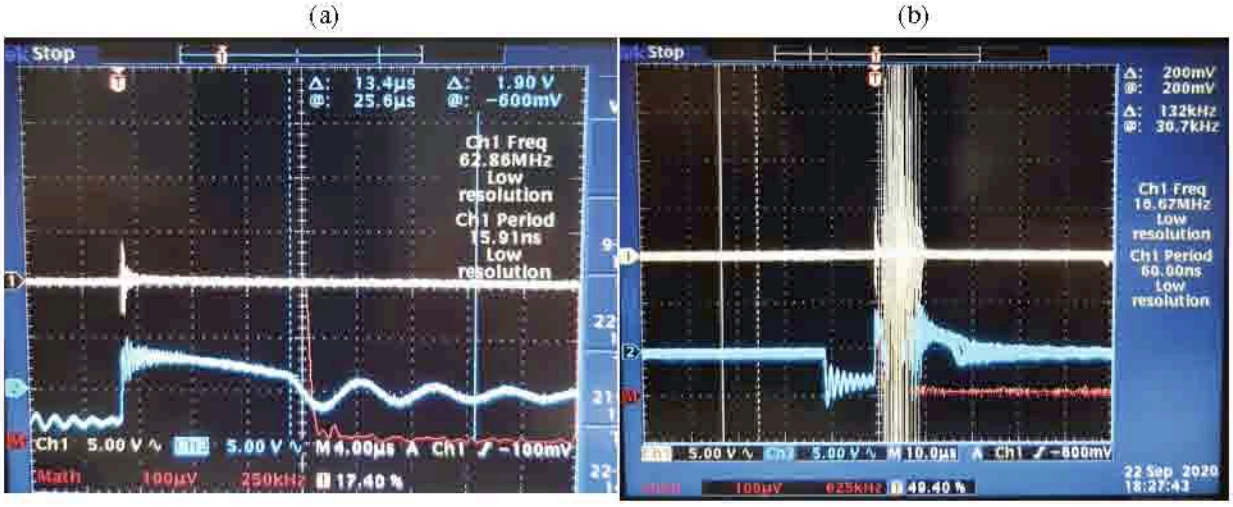

Fig. 5. Pulsed discharges in a deuterium medium with a palladium (Pd-D) sample: (a) (left) a single pulse, (1) $I = 4$ A, (2) $U \approx 2.5$ kV, and $f = 63$ MHz; (b) (right) an unstable discharge, consisting of a single discharge on the left side and a set of pulses with a current amplitude several times higher: (1) $I > 20$ A, (2) $U \approx 2.5$ kV, and $f = 17$ MHz.

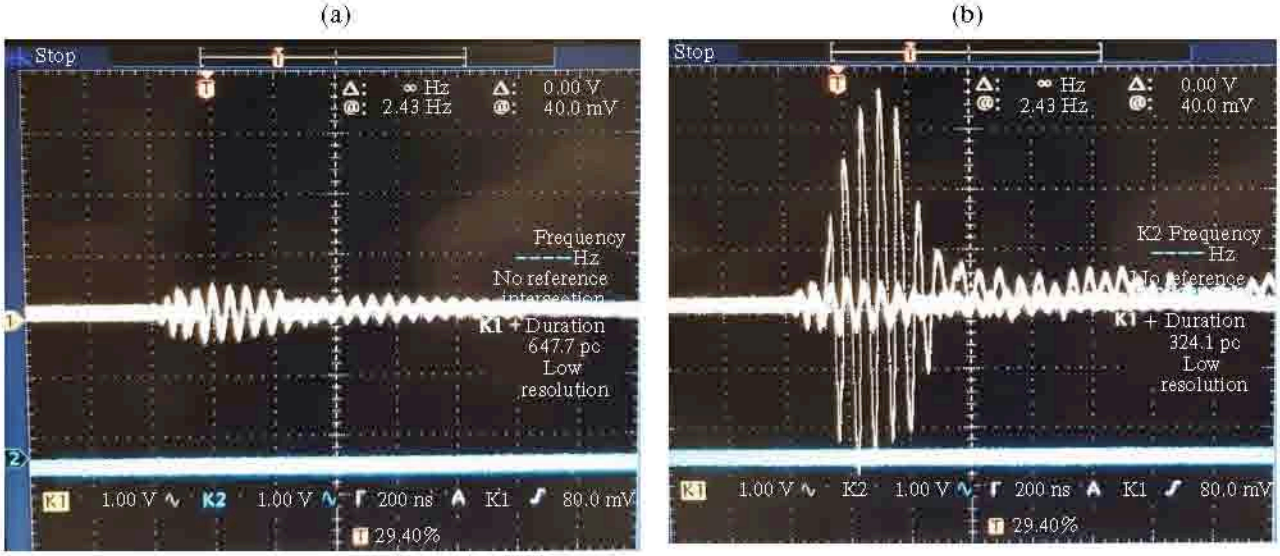

Fig. 6. Pulsed discharge in hydrogen on a nickel sample (Ni–H); (a) stable discharge: $I \approx 0.5$ A, $U \approx 0.5$ kV, and $f = 2.5$ MHz; (b) unstable discharge: formation (emergence) of additional higher intensity pulses: $I = (0.5–3.5)$ A, $U \approx 0.5$ kV, and $f = 1.25$ MHz.

Since, in mass spectrometric analysis, the identification of isotopes is associated with the $Z_i e/m_i$ ratio, the problems of identifying the mass m_i and establishing the cases of $Z_i \neq 1$ are much easier to solve when it comes to identifying an element that has several stable isotopes. In such cases—and we are analyzing just such a situation—one should focus on the known natural ratios of stable isotopes, which differ from the natural ones insignificantly, perhaps by several percent (usually less than 3–5%). This also makes it possible to separate the cases when the plasma contains isotopes with $Z_i \neq 1$. In our experiments, during the simultaneous analysis of several isotopes for each of the studied elements, such questions did not arise. Therefore, we did not have any problems with identifying isotopes and determining changes in the proportion of isotopes after glow-discharge treatment (and these changes could be significant).

It should be noted that, when analyzing the quantitative values of the masses of isotopes of an element and their ratios, we actually considered the contribution of all isotopes of each element, although the number of pulses detected for several masses is related with part of the pulses produced by isotopes of another ele-

Table 1. Ratio of Pd isotopes after irradiation in deuterium plasma

Pd		102*	104*	105	106	108	110
Natural content of isotope, %		1.02	11.14	22.33	27.33	26.46	11.72
Initial sample	%	1.03	10.85	21.81	26.76	26.92	12.62
	Number of pulses	3858790	40747202	81920014	100524262	101103042	47380042
After deuterium plasma	%	0.92	10.46	21.78	26.96	27.33	12.55
	Number of pulses	31593367	358917820	747400663	925107613	937807153	430371670
Multiplicity of increase in the number of pulses after D plasma*		8.2	8.8	9.1	9.2	9.3	9.1

* It is possible that part of the pulses with mass numbers 102 and 104 are produced by ruthenium isotopes $^{102}_{44}$Ru and $^{104}_{44}$Ru, but their number does not exceed 10^{-3} of the indicated numbers of pulses, as follows from the values of the pulses of the detected masses 99 and 101 and others corresponding to stable ruthenium isotopes.

ment. Specifically, in the case of Pd isotopes, we are talking about the masses 102 and 104 (Ru); for Pb isotopes in Pd, about mass 204 (Hg); and, for Pt isotopes in Pd, about 196 and 198 (Hg) masses. In the case of Ni isotopes, we are talking about masses 58 and 64; for Fe isotopes in Ni, about masses 54 (Cr) and 58 (Ni); and, for Zn isotopes in Ni, about masses 64 (Ni) and 70 (Ge). In the tables, all indicated masses are marked with asterisks and, in each case, immediately below the Table or in the text, the corresponding explanations are given. In all these cases, those were corrections that did not fundamentally change the conclusions following from the tables.

As for the accuracy of the measurements, the tables present the primary results: the number of pulses corresponding to the isotopes of each detected element obtained in one of three or four measurements carried out, as a rule, in different days. In all the cases considered, based on the obtained values N_{qi}, the relative fractions of each isotope i of the corresponding element q, normalized to unity, were determined for both the initial sample and the sample after the glow-discharge treatment. This procedure made it possible to reduce the statistical errors to the required level in a controlled manner. The relative root-mean-square deviation $\sigma_{qi} = \sqrt{N_{qi}}$ for the values of N_{qi} and the corresponding errors for the relative fractions of each ith isotope of an element q from the results of one measurement could be a priori calculated based on the obtained values of the counting rate of ions and the specified duration of measurements of one mass value. Statistical processing of the results of 15 consecutive measurements within the analysis of one sample allows one to obtain a posteriori estimate of the standard deviation.

The analysis shows that the statistical errors for the values of the recorded isotopic ratios in this case are small: local differences in the determined content of isotopes of each element in the surface layers of the studied palladium and nickel samples do not exceed 0.3% for the basic elements Pd and Ni and, for the impurity elements, range from fractions of a percent to 1–2% for a measurement duration of 1 second (tabulated data). At the same time, the spread of data for the detected elements in different parts of the studied cathodes, based on measurements carried out on different days, did not exceed 0.5% for the basic elements Pd and Ni and, for impurity elements, it could vary up to 3%. However, for our purpose of finding out the possibility of initiating—under the glow discharge conditions—nuclear processes leading to a significant (several times) decrease in the content of isotopes of impurity elements in the studied cathodes, such variations in the recorded local content of isotopes of impurity elements are insignificant.

3. EXPERIMENTAL RESULTS

3.1. Determining the Isotopic and Elemental Composition of a Palladium Sample

For the palladium sample considered in this paper, the data obtained in one of the experiments on the total values of N_{qi} for palladium isotopes and impurity elements Pt and Pb, on the initial fractions of each isotope in the sample under study, on the change in these fractions after exposure of the sample to a nonequilibrium glow-discharge plasma, and the abundance of the analyzed isotopes in nature are presented in Table 1 (for the isotopes of the basic element Pd) and in Tables 2 and 3 (for the impurity elements Pb and Pt in the Pd sample under study).

An order of magnitude greater number of pulses produced by isotopes of the main element Pd after treatment of the sample as a cathode in a glow discharge, which was already noted above, can be considered a consequence of the highly defective structure of the sample formed during such treatment, leading to an increase in the mass of samples (i.e., to a corresponding increase in the number of detected ions) during local destruction of the sample by laser abla-

Table 2. Reduction in the amount of Pb in the Pd cathode after irradiation in deuterium plasma

Pb in Pd		204*	206	207	208
Natural isotope content, %		1.4	24.1	22.1	52.4
Initial sample	%	1.5	24.6	19.7	54.2
	Number of pulses	12803*	215876	172365	474724
After deuterium plasma	%	6.3	23.7	20.0	50.1
	Number of pulses	Background **	1237	1044	2616
Remaining fraction of the isotope, %		< 0.1	<0.6	< 0.6	<0.5

*Here, we considered the number of pulses (413) related to the isotope $^{204}_{80}$Hg. The estimate was made from the number of pulses produced by the $^{200}_{80}$Hg isotope, assuming that the number of pulses is proportional to the natural content of the isotopes. The choice of another stable mercury isotope for this estimate does not fundamentally change the result.
**Number of pulses up to 50 are taken for background values.

Table 3. Reduction in the amount of Pt in the Pd cathode after irradiation in deuterium plasma

Pt in Pd		192	194	195	196*	198*
Natural isotope content, %		0.78	32.97	33.84	25.24	7.16
Initial sample	%	0.8	32.7	32.4	26.2	7.9
	Number of pulses	5700	245348	243489	197346	59343
After deuterium plasma	%	0.8	32.3	34.3	25.0	7.6
	Number of pulses	1760	69909	74229	54282	16492
Remaining fraction of the isotope, %		<30.9	<28.5	<30.5	<27.5	<27.8

*It is possible that part of the pulses are produced by isotopes $^{196}_{80}$Hg and $^{198}_{80}$Hg, but their number does not exceed 10^{-2} of the indicated numbers of pulses, as it follows from the numbers of detected masses of 200, 201, and others corresponding to stable mercury isotopes.

tion. Since we are primarily interested in the effect of a decrease in the initial content of impurity nonradioactive elements in the cathodes after their treatment in a glow-discharge plasma, the indicated increase in the mass of samples taken using the laser ablation method leads to some uncertainty in the decrease in the content (as a percentage of the initial amount) of impurity elements in the samples, recorded as "the remaining fraction of the isotope." This quantity is calculated as the ratio of the number of pulses corresponding to isotopes of impurity elements in the samples after treatment in the glow-discharge plasma and in the initial samples. Obviously, due to an increase in the mass of test materials taken from samples that have undergone plasma treatment, the real fraction of the impurity element remaining in the sample will be even smaller than the indicated value.

When presenting Table 1, we did not intend to understand the specific causes of small changes (on the order of a percent) in the content of isotopes of the basic element (palladium) after glow-discharge treatment of the cathode for 40 hours. The treatment time was chosen so that the integral flux of the formed neutrals $^2n_{isu}$ was sufficient to lead only to noticeable (several-fold!) changes in the content of impurity elements and, at the same time, in the relative proportion of their isotopes, without actually affecting the content of isotopes of the base element, which exceed the impurity content by orders of magnitude.

The results presented in Tables 1–3 indicate slight changes in the isotopic ratios in the main element Pd and somewhat greater isotopic changes in the impurity elements Pt and Pb under the action of a nonequilibrium low-temperature plasma. At the same time, the total amount of impurity elements Pt and Pb in the surface region of the original palladium sample is significantly reduced, which indicates the realization of nuclear processes in the near-surface region of the sample, leading to decay of the initially nonradioactive isotopes of Pt and Pb, i.e., to the manifestation of artificial radioactivity. In this case, the detected reduction in impurity lead isotopes is much more pronounced (the remainder is less than a percent of the initial content) than the reduction in the initial content of impurity platinum isotopes almost by a factor of three, also reliably detected.

These results cannot be understood within the existing concepts, dating back to I. Curie and F. Joliot (1934), according to which the decomposition of nonradioactive isotopes was considered possible only

Table 4. Ratios of isotopes $^{A}_{74}W$ in a Pd cathode after treatment in deuterium plasma and in a model tungsten sample

A		180	182	183	184	186
Natural isotope content, %		0.12	26.50	14.31	30.64	28.43
In the cathode after deuterium plasma	%	0.1	25.1	14.2	33.6	28.0
	Number of pulses 573217	704	143550	81442	192833	154688
In the cathode 4 months after deuterium plasma*	%	0.1	25.7	14.0	30.8	29.4
	Number of pulses 226944	272	58236	31673	69955	66808
On the opposite side of the cathode 4 months after deuterium plasma	%	0.1	25.4	13.7	29.7	31.1
	Number of pulses 106351	128	26955	14536	31640	33092
In the model W sample after deuterium plasma	%	0.1	25.5	14.2	30.8	29.4
	Number of impulses	135028	30267204	16857920	36560000	34819016

* The change in the total number of pulses in experiments four months after treatment, determined by a decrease in A^{tot} by a factor of ~2 in this case can be associated with relatively long-term uncontrolled relaxation changes in the near-surface region of the sample after 40 hours of treatment in plasma, including oxidative processes.

when they were bombarded with various particles, in particular, alpha-particles and protons of sufficiently high energies necessary to overcome the corresponding energy barriers and create radioactive nuclei in such collisions. Possible nuclear processes causing such artificial radioactivity under the conditions of our experiments will be discussed below in Section 5.

In particular, it will be shown that an important aspect for understanding the essence of the decay processes of initially nonradioactive isotopes Pt and Pb is the formation in the Pd cathode of all five isotopes (see Table 4), which are conventionally defined as stable due to their anomalously large half-lives $T_{1/2} \sim 10^{17}$–10^{19} years. In the initial Pd samples, tungsten impurities are insignificant, practically, at the background level. Therefore, Table 4 presents the number of pulses produced by all tungsten isotopes ($^{180}_{74}W$, $^{182}_{74}W$, $^{183}_{74}W$, $^{184}_{74}W$, and $^{186}_{74}W$) after glow-discharge treatment of the sample as a cathode, as well as the corresponding percentage of these isotopes. For comparison, the so-called "natural" ratios for these isotopes are also presented.

The appearance of tungsten isotopes in the Pd cathode could be associated with the use in the glow-discharge setup of a tungsten substrate, on which a palladium sample was placed on the cathode, since, under the glow-discharge conditions, tungsten from the substrate could diffuse into the Pd cathode. The data on the isotopic composition of tungsten of this substrate are also presented in Table 4, together with data on the presence of W isotopes and their isotopic ratios in the near-surface layer of the Pd cathode in contact with the tungsten substrate, i.e., from the side of the Pd sample that was not directly exposed to deuterium plasma. To obtain comparative information on the genesis of tungsten isotopes in the near-surface layers of the Pd cathode from the side of the action of plasma flows on it and from the opposite side, four months after the described experiment, data were obtained on the numbers of pulses produced by tungsten isotopes and the percentage of each isotope at both indicated interphase boundaries on the irradiated and unirradiated sides of the Pd cathode.

According to the data presented in Table 4, the content of W isotopes in the near-surface region of the Pd cathode from the side of the deuterium-containing plasma noticeably exceeds the content of W isotopes in the cathode from the side of the tungsten substrate. This unambiguously indicates that the formation of tungsten isotopes in the near-surface region of the cathode from the plasma side is not associated with the diffusion transfer of tungsten isotopes from the cathode–substrate interface. The only cause of the appearance of tungsten isotopes in the surface region of the cathode irradiated with ions may be linked with a detected reduction in the content of impurity Pt and Pb isotopes in the near-surface region of the original palladium sample under the action of deuterium-containing plasma. Moreover, the realization of nuclear reactions leading to the decay of Pt and Pb with formation of W isotopes is unambiguously indicated by the large differences in the relative content of isotopes, first of all, W-184 and W-186 in the Pd cathode from the side of the plasma after a 40-hour treatment of the cathode and in the model sample, about 3 and 2.5%, respectively. Four months after the experiments, these differences decrease and, directly in the

Table 5. Ni isotope ratio after irradiation in hydrogen plasma

Ni		58*	60	61	62	64*
Natural isotope content, %		68.08	26.22	1.14	3.63	0.93*
Initial sample	%	63.1	29.4	1.1	5.5	0.9
	Number of pulses	445460	207505	7470	38670	6563
After protium plasma	%	66.0	27.6	1.3	4.2	0.9
	Number of pulses	24555988	10275778	483529	1565551	346212
Multiplicity of increase in the number of pulses after H plasma		55.1	49.5	64.7	42.5	52.8

*See text for explanation.

Table 6. Reduction in Fe isotope content in Ni after irradiation in hydrogen plasma

Fe in Ni		54*	56	57	58*
Natural isotope content, %		5.85	91.70	2.12	0.28
In initial sample	%	6.4	91.1	2.2	0.3
	Total number of pulses	320951 (315234)	4472848	109286	13751
After protium plasma	%	18.7	79.4	1.6	0.3
	Total number of pulses	120542 (119614)	508803	10174	1793
Amount of remaining isotope, %		<37.6	<11.4	<9.3	<13.0

*See text for explanation.

surface layers of the cathode, these differences are about 0.3 and 1.5%.

3.2. Determining the Isotopic and Elemental Composition of a Nickel Sample

Experimental data on the total number of pulses for isotopes of the nickel sample and the impurity isotopes Fe, Zn, and Cu contained in the sample, on the initial percentage of each isotope in the nickel sample, on the change in the percentage of each isotope after exposure of the sample to nonequilibrium protium-containing glow-discharge plasma, as well as the abundance of the analyzed isotopes in nature are presented in Table 5 (for isotopes of the basic element Ni) and in Tables 6, 7, and 8 (for impurity elements Fe, Zn, and Cu in the sample Ni, respectively).

Tables 5–7 require explanation, since the elements listed there (marked with asterisks) have some isotopes of other elements with the same mass numbers; therefore, the total number of pulses corresponding to each such mass should be decomposed into parts corresponding to a specific element. To this end, first of all, we will assume that the fraction of isotopes whose natural content in the elements considered is small (of the order of 1% or less) and does not change after treatment in the plasma. It is natural to assume that possible changes in the content of such isotopes after plasma treatment will not greatly change the main estimates of our analysis, which substantiates the processes of initiated decay of initially nonradioactive isotopes after treatment in hydrogen-containing glow-discharge plasma. Here, we mean the Ni-64 and Fe-58 isotopes, the relative fractions of which among other nickel and iron isotopes, respectively, are 0.93 and 0.3%. The isolation of a relatively small number of pulses associated with the presence of Fe-58 in the sample, as well as the pulses produced by the Ni-64 isotope, is necessary not only to determine the number of pulses associated with the presence of the Ni-58 isotope, but also to refine the number of pulses associated with the presence of the Zn-64 isotope. But, to correct all the numbers of pulses produced by the nickel, iron, and zinc isotopes, it is necessary to refine the number of pulses associated with the Fe-54 isotope, since mass number 54 is also associated with the stable isotope Cr-54. The number of pulses associated with the latter isotope can be estimated based on the known numbers of signals associated with stable chromium isotopes, in particular, Cr-52, the natural fraction of which is 83.79%, because the natural fraction of the Cr-54 isotope among other stable chromium isotopes is relatively small, amounting to 2.36%. The corresponding recalculation of pulses characterizing the mass number 52 shows that the fraction of pulses corresponding to the Cr-54 isotope is less than 2% of the number of pulses characterizing the mass number

Table 7. Reduction in Zn isotope content in Ni after irradiation in hydrogen plasma

Zn in Ni		64*	66	67	68	70*
Natural isotope content, %		48.63	27.90	4.10	18.75	0.62
In initial sample	%	47.0	28.4	4.3	19.6	0.7
	Total number of pulses	8014649	4840528	741032	3347821	120765
After protium plasma	%	98.8	0.3	0.1	0.8	0.0
	Total number of pulses	437493	1404	578	3494	90
Amount of the remaining isotope, %		<5.5	<0.03	<0.08	<0.1	<0.07

*See text for explanation.

Table 8. Reduction in the number of Cu isotopes in Ni after treatment in hydrogen plasma

Cu in Ni		63	65	$^{63}Cu/^{65}Cu$
Natural isotope ratio, %		69.17	30.83	2.24
In initial sample	%	65.8	34.2	1.92
	Total number of pulses	230282834	119923026	
After protium plasma	%	68.4	31.6	2.16
	Total number of pulses	255329	118189	
Amount of remaining isotope, %		<0.1	<0.1	

for the Fe-54 isotope in Table 6. Considering these small corrections (they are enclosed in brackets in the column Fe-54 in Table 6) the sum of pulses corresponding to the Fe-54, Fe-56, and Fe-57 isotopes is determined, which, as indicated above, is 99.7% of the total number of pulses for this element. Hence, the number of pulses corresponding to Fe-58 is determined. Similarly, considering the number of pulses produced by Ni isotopes other than Ni-64 and by Zn isotopes other than Zn-70, the natural contents of which are 0.9 and 0.6%, respectively, the numbers of pulses corresponding to Ni-64 and Zn-70 are determined.

When analyzing the number of pulses associated with isotopes of impurity elements in samples obtained upon laser ablation, it should be borne in mind that the isotopes of impurity atoms in basic metal matrices (Pd and Ni in our case) are linked with matrices by less strong bonds than cohesive bonds between the base atoms. Therefore, it may be expected that the specific number of pulses per unit mass removed from the sample when "sampling" will be significantly smaller when analyzing the isotopes of the base samples.

The results presented in Tables 5–8 unambiguously indicate a change in isotopic ratios both in the main element Ni and in impurity elements under the action of a nonequilibrium low-temperature plasma on the sample. Moreover, the total amount of these impurity elements in the surface region of the initial nickel sample is significant, and some isotopes almost completely vanish, which indicates the realization of nuclear processes in the bulk of nickel, initiating the decay of all the presented initially nonradioactive isotopes of Fe, Zn, and Cu, i.e., artificial radioactivity. Therefore, a natural question arises of how the formation of radioactive isotopes from stable isotopes of iron, copper, and zinc can be initiated under the conditions of a low-temperature hydrogen-containing plasma. We will discuss this possibility below.

4. DISCUSSION OF RESULTS

4.1. Non-Nucleon Excitations of Atomic Nuclei under Conditions of Low-Temperature Plasma: Phenomenology

When discussing the possible causes of the changes occurring in the relative content of all identified isotopes under the action of low-temperature deuterium- and protium-containing glow-discharge plasma on palladium and nickel cathodes, we will use, as indicated in Introduction, the previously developed concepts [33–37] on the possibility of the formation of metastable nuclei (β nuclei) with a locally violated nucleon structure in a low-temperature plasma. Usually, when considering the mechanisms of nuclear processes and the decay of atomic nuclei ${}^{A}_{Z}N$ (Z and A are the atomic and mass number of a nucleus N, respectively), nuclear matter is represented in the form of interacting nucleons. However, under conditions of a nonequilibrium low-temperature plasma in the presence of electrons in the plasma with a sufficiently large

(on the chemical scales) kinetic energy $E_e \sim 3$–5 eV, the situation may be different.

It is known that during K-capture, when the electron of the inner shells of the atom interacts with the surface of the nucleus and a new, daughter nucleus is formed, the nucleon structure of nuclear matter does not change. At the initial, irreversible stage of this process, the electron, when interacting with the surface of the nucleus, emits a neutrino ν. The resulting virtual vector W^- boson, incorporated in nuclear matter, when interacting with a u quark of one of the protons turns into a d quark, as a result of which this proton turns into a neutron, which results in the formation of a nucleus ${}^{A}_{Z-1}M$. However, if the plasma contains atoms in which K-capture in a nucleus is forbidden (it is exactly these cases that are considered below) and the process of ionization of the electron shells of atoms by electrons with a kinetic energy $E_e \sim 3$–5 eV is not yet realized, then the scattering of such electrons (their de Broglie wave $\lambda \approx 0.6$ nm) on atoms and ions initiates vibrational dynamics of the electronic subsystems of atoms and ions and, consequently, an increase in the probability of the interaction of electrons of the inner subshells of atoms and ions with the corresponding nuclei.

At the first, irreversible, stage of such a nuclear-chemical interaction, a neutrino ν is emitted and a vector W^- boson incorporates into the nuclear matter of the original nucleus ${}^{A}_{Z}N$ in accordance with

$$ {}^{A}_{Z}N + e^-_{he} \rightarrow {}^{A}_{Z-1}M_{isu} + \nu. \quad (1) $$

The subscript (high energy) in the designation of an electron on the left-hand side of (1) indicates the activated character of this stage of the process, and the subscript in the designation of the nucleus on the right-hand side of relation (1) indicates the formation in such a process of nuclei ${}^{A}_{Z-1}M_{isu}$ in the metastable state ("inner shake-up" or isu-state) of nuclear matter with a locally disturbed nucleon structure. Indeed, the vector W^- boson interacting with the u quark of one of the protons of the nucleus ${}^{A}_{Z}N$ can only produce a virtual d quark, but the three quarks that have emerged from the proton—two d quarks and a u quark—cannot form a neutron due to the lack of total mass of such a kernel for K-capture. The initiated chain of virtual transformations of quarks with the participation of vector W bosons in the formed nucleus with a distorted nucleon structure must be interrupted by irreversible decay of the virtual W^- boson with the formation of the initial nucleus, electron, and antineutrino $\tilde{\nu}$:

$$ {}^{A}_{Z-1}M_{isu} \rightarrow {}^{A}_{Z}N + e^- + \tilde{\nu}, \quad (2) $$

so that the total process with the corresponding stages (1) and (2) is represented in the form of inelastic scattering of an electron by the initial nucleus in the channel of weak nuclear interaction:

$$ {}^{A}_{Z}N + e^-_{he} \rightarrow {}^{A}_{Z}N + e^- + \nu + \tilde{\nu}. \quad (3) $$

Nuclei with a state of nuclear matter in a metastable isu-state will be defined as β nuclei. The threshold energy of such a process with the creation of a $\nu\,\tilde{\nu}$ pair, determined by the neutrino–antineutrino rest masses, is about 0.3 eV [39].

The formation in the nucleus of three quarks not bound into a nucleon, which, in this case, can be considered to be "markers" of new degrees of freedom, in fact, means that the intensity of nuclear forces is insufficient to provide the conventional, proton–neutron organization of nuclear matter in the system. The subsequent relaxation dynamics of the locally arisen isu-state, which can be transferred by means of pions to other nucleons of the nucleus, is initiated only by weak nuclear interactions, which are realized through quarks during the production and absorption of gauge vector neutral Z^0 and charged $W^{\pm}$ bosons. The lifetime of the formed β nuclei in the metastable isu state, as follows from a specially designed experiment [31] on the synthesis of tritium during laser ablation of metals in heavy water and experimental results on the initiated decay of U-238 [35, 36], may be rather significant, from tens of minutes to several years, and nuclei in this state can directly participate in various nuclear processes [33, 34], including nucleosynthesis in the stars [37, 40].

It should also be borne in mind that the relaxation rearrangement of nuclear matter during the formation of products of such nuclear transformations proceeds primarily through the formation of a purely nucleon structure of the nucleus, in accordance with the principle of least action. In nuclei with a proton–neutron, nucleon structure, excitation–relaxation processes can go through the excited states of the nucleus and include the stages of emission of γ quanta, whereas, in nuclei with a partial "nonnucleon" state of nuclear matter, such relaxation is almost excluded and the relaxation of the resulting products is inevitably associated with the loss of energy through the emission of neutrino–antineutrino pairs, or the URCA process [41]. That is why the associated nuclear processes turn out to be safe.

It is worth noting some unexpectedness of the result presented above about the possibility of external effect of electrons on the dynamics of decay of a radioactive nucleus. It turns out that, although electrons cannot interact with nucleons of the nucleus as fragments of nuclear matter, they can initiate (via vector W^- bosons) local disturbances in the nucleon structure of the nucleus. At the same time, as experience shows, external excitations of a radioactive nucleus as an integral system (under the action of γ radiation, in particular) cannot affect the rate of radioactive decay, and, consequently, the phenomenon of initiation of

nuclear instability discussed here. In these cases, nuclear matter manifests itself as an integral system of interacting nucleons with their inherent individual characteristics.

With regard to the problems of initiation of artificial radioactivity considered in this work, we will be interested in the simplest of β nuclei, which are β neutron ${}^{1}n_{isu}$ and β dineutron ${}^{2}n_{isu}$. These nuclei are formed by the interaction of high-energy electrons with protons ${}^{1}_{1}H$ or deuterons ${}^{2}_{1}H$ under the conditions of protium- or deuteron-containing glow-discharge plasma, respectively, according to:

$$ {}^{1}_{1}H + e^{-}_{he} \rightarrow {}^{1}n_{isu} + \nu, \quad (4) $$

$$ {}^{2}_{1}H + e^{-}_{he} \rightarrow {}^{2}n_{isu} + \nu. \quad (5) $$

If the half-lives $T_{1/2}$ of such β nuclei are long enough, neutral nuclei ${}^{1}n_{isu}$ and ${}^{2}n_{isu}$, formally characterized, respectively, by baryon numbers equal to one and two, zero lepton charges, and rest masses equal to the masses of the hydrogen and deuterium atoms, can effectively participate in various nuclear processes.

This conclusion is based on the results of a number of works on the "cold synthesis" of a number of elements, in particular, gold upon laser ablation of mercury-196 in heavy water [29] and tritium upon laser ablation of a number of metals in heavy water [31]. During the synthesis of tritium, its activity in heavy water exceeded the background activity of the initial system by three orders of magnitude when the cathodic bias was applied to the metals used. Such results could be understood by assuming that the half-life $T_{1/2}$ of the β dineutron subject to decay

$$ {}^{2}n_{isu} \rightarrow {}^{2}_{1}H + e^{-} + \tilde{\nu} \quad (6) $$

with the formation of a deuteron ${}^{2}_{1}H$, an electron, and an antineutrino, turns out to be rather long, at least tens of minutes. It was assumed that the actual process of production of tritium ${}^{3}_{1}H$ occurred during the interaction of a deuteron ${}^{2}_{1}H$ with a nucleus ${}^{2}n_{isu}$:

$$ {}^{2}_{1}H + {}^{2}n_{isu} \rightarrow {}^{3}_{1}H + n + Q(3.25\ \text{MeV}), \quad (7) $$

where n is a neutron.

The authors of [31] also postulated the possibility of the production of a hypothetical β trineutron ${}^{3}n_{isu}$ during the interaction of electrons with tritium nuclei ${}^{3}_{1}H$:

$$ {}^{3}_{1}H + e^{-}_{he} \rightarrow {}^{3}n_{isu} + \nu, \quad (8) $$

The rest mass of the introduced neutral nucleus ${}^{3}n_{isu}$ was assumed to be equal to the rest mass of the tritium atom. It is through the formation of a nucleus ${}^{3}n_{isu}$ that the process, discovered in [31], of initiated decay of tritium nuclei under the conditions of laser ablation of metals in aqueous media, along with the synthesis of tritium nuclei, can proceed. The corresponding gross process can be represented as

$$ {}^{3}_{1}H + e^{-}_{he} \rightarrow {}^{3}n_{isu} + \nu $$
$$ \rightarrow {}^{3}_{2}He + 2e^{-} + \nu + 2\tilde{\nu} + Q(0.019\ \text{MeV}). \quad (9) $$

It should be noted that the half-life $T_{1/2}$ of the nucleus ${}^{3}n_{isu}$, according to [31], is of the same order of magnitude as the half-life of the nucleus ${}^{2}n_{isu}$, which is many orders of magnitude smaller than the half-life of the tritium nucleus ($T_{1/2}$ = 12.3 years).

Meanwhile, it can be argued that it is the introduction of the concept of rather long-lived neutral β nuclei ${}^{1}n_{isu}$ and ${}^{2}n_{isu}$, which are produced in protium- and deuterium-containing glow-discharge plasma, respectively, and are capable of quite effectively penetrating into the near-surface defect layers of palladium and nickel cathodes, that made it possible to understand what type of nuclear processes could cause a significant reduction in the content of impurity nonradioactive elements detected in the experiments. It should be emphasized here that, in contrast to nuclear reactions occurring during collisions of reactants in the gas phase, for the considered nuclear transformations in the region of grain boundaries of the solid phase of metals, due to the possible influence of the environment, the energy factor alone is sufficient (without spin and parity matching of colliding and final nuclei). In nuclear processes involving ${}^{1}n_{isu}$ and ${}^{2}n_{isu}$ particles, when the fusion of nuclear matter of the initial stable nucleus with the nuclear matter of the aforementioned neutral light nuclei in the isu-state, in addition to the total excitation energy of the "compound nucleus," which, in the cases under consideration, is about 10 MeV relative to the ground state of the indicated nuclei, the nuclear matter of such nuclei can be partially in an unbalanced isu-state with the loss of the stability of the nucleus.

In this case, the compound nucleus actually turns out to be radioactive and it will face an inevitable transformation. It is assumed that the nuclear structure is rearranged during the decay of a compound nucleus through the weak nuclear interactions with the relaxation dynamics of URCA processes upon emission of $\nu\tilde{\nu}$ pairs, which leads to the complete absence of hazardous radiation. No specific a priori estimates of the decay probabilities of such compound nuclei can be made, including processes with the simultaneous emission of alpha particles and electrons, since the decay processes of excited nuclei with a disturbed nucleon structure of the type under consideration have not previously been considered in nuclear physics. Therefore, the only basis for the possible mechanisms of the processes observed has been the direct mass spectrometric information on changes

in the elemental and isotopic composition of the main impurities in Pd and Ni cathodes and the appearance, in the case of a Pd cathode, of tungsten isotopes as an impurity, as well as the absence of ionizing radiation. The characteristic time of this transformation must be determined by many factors, both purely energetic and, possibly, structural, meaning the admissible rearrangements in the nuclear matter of the compound nucleus. The analysis of the dynamics of radioactive decay of a nucleus can involve the Kramers activation process in its discrete version ("wandering" over energy levels with reaching a certain boundary) [42, 43], which is widely used in physicochemical kinetics. Here, we mean the dynamics of energy accumulation by the nucleus in the unstable isu-state at the "last" bond, the breaking of which means the decay of the nucleus along a certain channel. Possible paths of nuclear-chemical reactions that determine the decay processes of impurity elements in palladium and nickel electrodes under glow-discharge conditions in this study are discussed in the next section.

4.2. Possible Mechanisms of Nuclear-Chemical Reactions Involving Impurity Elements in Palladium and Nickel Cathodes

4.2.1 Palladium cathode. Palladium cathode containing Pb and Pt impurity elements during a glow discharge in a deuterium-containing gas environment. We will assume, in accordance with the previous section, that, in the interaction of neutral nuclei $^2n_{isu}$ with the nuclei of the elements under consideration in the process of fusion of the nuclear matter of these nuclei, a compound nucleus is formed in an excited state (marked with an asterisk in the upper right corner in the notation used for this nucleus) and the total energy of the resulting nucleus is redistributed over its volume by means of Z^0 vector bosons, initiating the formation of the nucleon structure of the daughter nuclei and the emission of part of the energy in the form of $\nu\tilde{\nu}$ pairs in accordance with the laws of conservation of energy and momentum. Naturally, under conditions of the action of plasma flows on a palladium electrode, the $^2n_{isu}$ nuclei mainly interact with palladium isotopes. These are the processes of mutual transformations of stable isotopes:

$$^{A}_{46}\mathrm{Pd} + {}^{2}\mathrm{n}_{isu} \rightarrow {}^{A+2}_{46}\mathrm{Pd}^{*}_{isu} \rightarrow {}^{A+2}_{46}\mathrm{Pd} + \nu\tilde{\nu} + Q_A, \quad (10)$$

where A = 102, 104, 106, and 108 and the energy release values during the production of isotopes with mass numbers A = 104, 106, 108, and 110 are, respectively, Q_A = 14.60, 13.65, 12.75, and 11.96 MeV, as well as

$$^{A}_{46}\mathrm{Pd} + {}^{2}\mathrm{n}_{isu} \rightarrow {}^{A+2}_{46}\mathrm{Pd}^{*}_{isu} \rightarrow {}^{4}_{2}\mathrm{He} + {}^{A-2}_{46}\mathrm{Pd} + 2e^{-} + 2\tilde{\nu} + \nu\tilde{\nu} + Q_A, \quad (11)$$

where A = 104, 106, 108, and 110, and the energy release values during the production of isotopes with mass numbers A = 102, 104, 106, and 108 are, respectively, Q_A = 9.25, 10.20, 10.99, and 11.75 MeV.

Upon the interaction of neutral nuclei $^2n_{isu}$ with palladium isotopes, new elements can also be produced. Here are some examples of such possible reactions:

$$^{105}_{46}\mathrm{Pd} + {}^{2}\mathrm{n}_{isu} \rightarrow {}^{107}_{46}\mathrm{Pd}^{*}_{isu} \rightarrow {}^{4}_{2}\mathrm{He} + {}^{103}_{45}\mathrm{Rh} + e^{-} + \tilde{\nu} + \nu\tilde{\nu} + Q(10.32\ \mathrm{MeV}), \quad (12)$$

$$^{A}_{46}\mathrm{Pd} + {}^{2}\mathrm{n}_{isu} \rightarrow {}^{A+2}_{46}\mathrm{Pd}^{*}_{isu} \rightarrow {}^{4}_{2}\mathrm{He} + {}^{A-2}_{44}\mathrm{Ru} + \nu\tilde{\nu} + Q_A, \quad (13)$$

where A = 102, 104, and 106, and the values of the energy release for the indicated A during the formation of ruthenium isotopes 102, 104, and 106 are, respectively, Q_A = 12.00, 10.42, and 8.9 MeV. Regarding the processes with the production of ruthenium, it is difficult to draw unambiguous conclusions about the manifestation of such processes in the analysis of the mass spectra obtained, since the masses of the indicated ruthenium isotopes 100, 102, and 104 can be associated with isotopes of other elements (Mo-100, Pd-102, and Pd-104). At the same time, the mass number 103 can be associated only with rhodium, with which, during the mass spectral analysis, 7621 pulses were associated in the initial sample and 28136 pulses after glow-discharge treatment of the palladium sample. Naturally, it is impossible to separate the contribution of such numbers of pulses against the background of pulses associated with the Pd-105 isotope, which are greater by orders of magnitude.

Let us consider further possible processes for the $^2n_{isu}$ nuclei with isotopes of the impurity elements lead and platinum. In the case of lead, the reactions of the production of its heavier isotopes are presented in the form

$$^{A}_{82}\mathrm{Pb} + {}^{2}\mathrm{n}_{isu} \rightarrow {}^{A+2}_{82}\mathrm{Pb}^{*}_{isu} \rightarrow {}^{A+2}_{82}\mathrm{Pb} + \nu\tilde{\nu} + Q_A. \quad (14)$$

Here, A = 204 and 206 and the values of energy release Q_A during the formation of isotopes with mass numbers A = 206 and 208 are Q_A = 11.81 and 11.10 MeV, respectively. Simultaneously, reactions with the production of lighter isotopes,

$$^{A}_{82}\mathrm{Pb} + {}^{2}\mathrm{n}_{isu} \rightarrow {}^{A+2}_{82}\mathrm{Pb}^{*}_{isu} \rightarrow {}^{4}_{2}\mathrm{He} + {}^{A-2}_{82}\mathrm{Pb} + 2e^{-} + 2\tilde{\nu} + \nu\tilde{\nu} + Q_A, \quad (14a)$$

can also take place. Here, A = 206 and 208 and the values of energy release during the formation of isotopes with mass numbers A = 204 and 206 are equal to Q_A = 12.03 and 12.75 MeV, respectively.

Let us give examples of processes resulting in a decrease in the content of lead isotopes in the palladium cathode under the action of flows of a deuteron-containing glow-discharge plasma. If we focus on the values of energy release in nuclear processes initiated by the interaction of $^{2}n_{isu}$ nuclei with lead isotopes, then the main daughter products in such processes are platinum isotopes, which, along with lead isotopes, are also detected as an impurity in the initial palladium samples:

$$^{A}_{82}\mathrm{Pb} + {}^{2}n_{isu} \rightarrow {}^{A+2}_{82}\mathrm{Pb}^{*}_{isu} \rightarrow {}^{12}_{6}\mathrm{C} + {}^{A-10}_{78}\mathrm{Pt} + 2e^{-} + 2\tilde{\nu} + \nu\tilde{\nu} + Q_{A} \quad (15)$$

(here, for $A = 204$, 206, and 208, the values of the energy release Q_A during the production of isotopes with mass numbers 194, 196, and 198 are, respectively, $Q_A = 22.79$, 21.00, and 21.29 MeV);

$$^{206}_{82}\mathrm{Pb} + {}^{2}n_{isu} \rightarrow {}^{208}_{82}\mathrm{Pb}^{*}_{isu} \rightarrow {}^{13}_{6}\mathrm{C} + {}^{195}_{78}\mathrm{Pt} + 2e^{-} + 2\tilde{\nu} + \nu\tilde{\nu} + Q(19.02\ \mathrm{MeV}); \quad (16)$$

$$^{A}_{82}\mathrm{Pb} + {}^{2}n_{isu} \rightarrow {}^{A+2}_{82}\mathrm{Pb}^{*}_{isu} \rightarrow {}^{16}_{8}\mathrm{O} + {}^{A-14}_{78}\mathrm{Pt} + 4e^{-} + 4\tilde{\nu} + \nu\tilde{\nu} + Q_{A} \quad (16a)$$

(here, for $A = 204$ and 206, the values of the energy release during the formation of Pt isotopes with mass numbers 190 and 192 are $Q_A = 30.07$ and 30.37 MeV, respectively).

In the case of platinum, the reactions of the production of its heavier isotopes are represented as

$$^{A}_{78}\mathrm{Pt} + {}^{2}n_{isu} \rightarrow {}^{A+2}_{78}\mathrm{Pt}^{*}_{isu} \rightarrow {}^{A+2}_{78}\mathrm{Pt} + \nu\tilde{\nu} + Q_{A}. \quad (17)$$

Here, $A = 190$, 192, 194, and 196 and the values of energy release Q_A during the formation of isotopes with mass numbers $A = 192$, 194, 196, and 198 are $Q_A = 12.11$, 11.62, 11.02, and 10.40 MeV, respectively. Simultaneously, reactions of the formation of lighter isotopes,

$$^{A}_{78}\mathrm{Pt} + {}^{2}n_{isu} \rightarrow {}^{A+2}_{78}\mathrm{Pt}^{*}_{isu} \rightarrow {}^{4}_{2}\mathrm{He} + {}^{A-2}_{78}\mathrm{Pt} + 2e^{-} + 2\tilde{\nu} + \nu\tilde{\nu} + Q_{A}, \quad (17a)$$

can also take place, where $A = 192$, 194, 196, and 198 and the values of energy release during the formation of isotopes with mass numbers $A = 190$, 192, 194, and 196 are $Q_A = 11.74$, 12.23, 12.83, and 13.45 MeV, respectively.

By inspecting numbers on the energy release in nuclear reactions of the $^{2}n_{isu}$ nuclei with impurity platinum isotopes, it can be assumed that the main processes causing the reduction in platinum isotopes during the treatment of palladium samples in a glow-discharge plasma are nuclear reactions with the formation of tungsten isotopes:

$$^{195}_{78}\mathrm{Pt} + {}^{2}n_{isu} \rightarrow {}^{197}_{78}\mathrm{Pt}^{*}_{isu} \rightarrow {}^{14}_{7}\mathrm{N} + {}^{183}_{74}\mathrm{W} + 3e^{-} + 3\tilde{\nu} + \nu\tilde{\nu} + Q(23.83\ \mathrm{MeV}); \quad (18)$$

$$^{198}_{78}\mathrm{Pt} + {}^{2}n_{isu} \rightarrow {}^{200}_{78}\mathrm{Pt}^{*}_{isu} \rightarrow {}^{14}_{7}\mathrm{N} + {}^{186}_{74}\mathrm{W} + 3e^{-} + 3\tilde{\nu} + \nu\tilde{\nu} + Q(22.96\ \mathrm{MeV}); \quad (19)$$

$$^{A}_{78}\mathrm{Pt} + {}^{2}n_{isu} \rightarrow {}^{A+2}_{78}\mathrm{Pt}^{*}_{isu} \rightarrow {}^{12}_{6}\mathrm{C} + {}^{A-10}_{74}\mathrm{W} + 2e^{-} + 2\tilde{\nu} + \nu\tilde{\nu} + Q_{A}, \quad (20)$$

where $A = 190$, 192, 194, and 196 and the values of energy release for the indicated A during the production of the tungsten-180, 182, 184, and 186 isotopes are, respectively, 25.45, 25.09, 24.06, and 22.98 MeV.

The data presented in Section 3.1 and Table 4 on the production of tungsten isotopes in the Pd cathode after treatment in a deuterium-containing plasma are formally quite consistent with the assumption made. In this case, however, a question arises. The W-184 and -186 isotopes, the relative fractions of which are 33.64 and 26.66%, respectively, are produced, in accordance with (20) and (19), in nuclear processes involving the Pt-196 and Pt-198 isotopes, the relative fractions of which among the platinum isotopes are 26.7 and 7.90%. The question is why the 3-fold difference in the proportions of platinum isotopes does not actually appear, so that, in the final product, the proportions of the W-184 and W-186 isotopes turn out to be close. Moreover, as follows from (19) and (20), the probability of the reaction with the production of the W-186 isotope should be even lower than the probability of the production of the W-184 isotope, due to the smaller phase space in the case of the reaction with the production of three electrons and antineutrinos, rather than reactions with the formation of two electrons and an antineutrino.

We believe that, to answer this question, it is necessary to consider the problem in its most general form, namely, to take into account the formation of platinum isotopes in processes (15) under the action of deuterium-containing plasma on the impurity lead nuclei, primarily, Pb-206 (215876) and Pb-208 (474724), since it is with these isotopes that the production of the Pt-196 (197346) and Pt-198 (59343) isotopes is associated; then, the subsequent formation of the W-184 (192833) and W-186 (154688) isotopes should be considered in accordance with indicated processes (20) and (19). As noted above, the numbers of pulses given in parentheses for each isotope, taken from Tables 2–4, are regarded as a quantitative characteristic of the total amount of a given isotope of each specific element contained in the Pd cathode. It is the comparative analysis of the quantitative characteristics that allows us to conclude that the production of the indicated tungsten isotopes, in particular, W-184 and

W-186, in the ratios found in the analysis, requires a "feed" of the Pd cathode with the Pt-196 and Pt-198 isotopes, i.e., the participation of the Pb-206 and Pb-208 isotopes in the processes. Moreover, as follows from processes (14a), (15), (16), and (16a), during the considered initiated decays of the heaviest lead isotopes, the Pd cathode is fed with lighter platinum isotopes: Pt190, Pt-192, Pt-194, and Pt-195 and the general dynamism of the processes under consideration is maintained by mutual transformations of lead and platinum isotopes in accordance with reactions (14) and (14a), as well as (17) and (17a). Therefore, an important factor determining the establishment in the Pd cathode after treatment not only of a relatively high fraction of the W-186 isotope but relative fractions of other tungsten isotopes produced there, is the high fraction (54.18%) of Pb-208 relative to other lead isotopes.

4.2.2 Nickel cathode. Nickel cathode containing Cu, Zn, and Fe impurity elements in a glow discharge in a protium-containing gaseous medium. Under the action of flows of a protium-containing low-temperature glow-discharge plasma on a nickel cathode, neutral nuclei formed in reaction (4) turn out to be the main factor initiating nuclear-chemical processes in the cathode. First of all, these are the processes of some mutual transformations of stable isotopes:

$$ {}^{A}_{28}\mathrm{Ni} + {}^{1}\mathrm{n}_{isu} \rightarrow {}^{A+1}_{28}\mathrm{Ni}^{*}_{isu} \rightarrow {}^{A+1}_{28}\mathrm{Ni} + \nu\tilde{\nu} + Q_A, \quad (21) $$

where $A = 60$ and 61 and the values of energy release during the production of nickel isotopes with mass numbers $A = 61$ and 62 are, respectively, $Q_A = 7.04$ and 9.81 MeV;

$$ \begin{gathered} {}^{A}_{28}\mathrm{Ni} + {}^{1}\mathrm{n}_{isu} \rightarrow {}^{A+1}_{28}\mathrm{Ni}^{*}_{isu} \\ \rightarrow {}^{4}_{2}\mathrm{He} + {}^{A-3}_{28}\mathrm{Ni} + 2\mathrm{e}^{-} + 2\tilde{\nu} + \nu\tilde{\nu} + Q_A, \end{gathered} \quad (22) $$

where $A = 61$ and 64 and the values of energy release during the production of nickel isotopes with mass numbers $A = 58$ and 61 are $Q_A = 0.87$ and 2.42 MeV, respectively, as well as the processes of obtaining stable isotopes of other elements from nickel isotopes:

$$ \begin{gathered} {}^{A}_{28}\mathrm{Ni} + {}^{1}\mathrm{n}_{isu} \rightarrow {}^{A+1}_{28}\mathrm{Ni}^{*}_{isu} \\ \rightarrow {}^{A+1}_{29}\mathrm{Cu} + \mathrm{e}^{-} + \tilde{\nu} + \nu\tilde{\nu} + Q_A, \end{gathered} \quad (23) $$

where $A = 62$ and 64 and the values of energy release during the formation of copper isotopes with mass numbers $A = 63$ and 65 are, respectively, $Q_A = 6.12$ and 2.95 MeV.

Let us now consider the processes that cause the reduction in the content of isotopes of impurity non-radioactive elements: copper, zinc, and iron in nickel cathodes during a 40-hour treatment in a protium-containing glow-discharge plasma under the action of neutral nuclei ${}^{1}\mathrm{n}_{isu}$ on the nickel ions. Apparently, the main processes leading to a reduction in the copper content in nickel samples can be represented as follows:

$$ \begin{gathered} {}^{63}_{29}\mathrm{Cu} + {}^{1}\mathrm{n}_{isu} \rightarrow {}^{64}_{29}\mathrm{Cu}^{*}_{isu} \\ \rightarrow {}^{64}_{30}\mathrm{Zn} + \mathrm{e}^{-} + \tilde{\nu} + \nu\tilde{\nu} + Q(7.71\ \mathrm{MeV}), \end{gathered} \quad (24) $$

$$ \begin{gathered} {}^{65}_{29}\mathrm{Cu} + {}^{1}\mathrm{n}_{isu} \rightarrow {}^{66}_{29}\mathrm{Cu}^{*}_{isu} \\ \rightarrow {}^{66}_{30}\mathrm{Zn} + \mathrm{e}^{-} + \tilde{\nu} + \nu\tilde{\nu} + Q(8.92\ \mathrm{MeV}). \end{gathered} \quad (25) $$

It can be assumed that a higher level of reduction in the content of copper-65 in the nickel cathode under the action of plasma flows, as follows from the ratio ${}^{63}\mathrm{Cu}/{}^{65}\mathrm{Cu}$ (Table 8), is determined by the higher energy release in process (25) compared to process (24). Below, we present reactions involving zinc isotopes, in which helium and both copper isotopes are produced, which must have a lower probability due to the lower energy release and phase spaces of these processes.

Let us present the main processes that determine the reduction in the content of stable zinc isotopes in a nickel cathode. We assume that the interaction of the Zn-64 nucleus with the ${}^{1}\mathrm{n}_{isu}$ nucleus and the production of the compound Zn-65 nucleus in the isu-state initiates the interaction of the K-shell electron with this nucleus (it is known that the Zn-65 nucleus undergoes K-capture in the ground state), leading to the formation a Cu-65 nucleus, which can be represented as a gross process

$$ \begin{gathered} {}^{64}_{30}\mathrm{Zn} + {}^{1}\mathrm{n}_{isu} \rightarrow {}^{65}_{30}\mathrm{Zn}^{*}_{isu} \\ \xrightarrow[+\mathrm{e}^{-}]{} {}^{65}_{29}\mathrm{Cu} + \nu + \nu\tilde{\nu} + Q(8.55\ \mathrm{MeV}). \end{gathered} \quad (26) $$

The other processes can be represented as

$$ \begin{gathered} {}^{66}_{30}\mathrm{Zn} + {}^{1}\mathrm{n}_{isu} \rightarrow {}^{67}_{30}\mathrm{Zn}^{*}_{isu} \\ \rightarrow {}^{67}_{30}\mathrm{Zn} + \nu\tilde{\nu} + Q(6.27\ \mathrm{MeV}), \end{gathered} \quad (27) $$

$$ \begin{gathered} {}^{67}_{30}\mathrm{Zn} + {}^{1}\mathrm{n}_{isu} \rightarrow {}^{68}_{30}\mathrm{Zn}^{*}_{isu} \\ \rightarrow {}^{68}_{30}\mathrm{Zn} + \nu\tilde{\nu} + Q(9.42\ \mathrm{MeV}), \end{gathered} \quad (28) $$

$$ \begin{gathered} {}^{68}_{30}\mathrm{Zn} + {}^{1}\mathrm{n}_{isu} \rightarrow {}^{69}_{30}\mathrm{Zn}^{*}_{isu} \\ \rightarrow {}^{4}_{2}\mathrm{He} + {}^{65}_{29}\mathrm{Cu} + \mathrm{e}^{-} + \tilde{\nu} + \nu\tilde{\nu} + Q(7.97\ \mathrm{MeV}), \end{gathered} \quad (29) $$

$$ \begin{gathered} {}^{68}_{30}\mathrm{Zn} + {}^{1}\mathrm{n}_{isu} \rightarrow {}^{69}_{30}\mathrm{Zn}^{*}_{isu} \\ \rightarrow {}^{69}_{31}\mathrm{Ga} + \mathrm{e}^{-} + \tilde{\nu} + \nu\tilde{\nu} + Q(6.61\ \mathrm{MeV}), \end{gathered} \quad (30) $$

$$ \begin{gathered} {}^{70}_{30}\mathrm{Zn} + {}^{1}\mathrm{n}_{isu} \rightarrow {}^{71}_{30}\mathrm{Zn}^{*}_{isu} \\ \rightarrow {}^{71}_{31}\mathrm{Ga} + \mathrm{e}^{-} + \tilde{\nu} + \nu\tilde{\nu} + Q(7.87\ \mathrm{MeV}). \end{gathered} \quad (31) $$

Despite the production of gallium isotopes in processes (30) and (31), the accumulation of these isotopes in the nickel cathode does not occur, since both

isotopes can effectively participate in the following transformations:

$$^{69}_{31}\mathrm{Ga} + {}^{1}\mathrm{n}_{\mathrm{isu}} \rightarrow {}^{70}_{31}\mathrm{Ga}^{*}_{\mathrm{isu}} \rightarrow {}^{70}_{32}\mathrm{Ge} + \mathrm{e}^{-} + \tilde{\nu} + \nu\tilde{\nu} + Q(8.53\ \mathrm{MeV}), \quad (32)$$

$$^{71}_{31}\mathrm{Ga} + {}^{1}\mathrm{n}_{\mathrm{isu}} \rightarrow {}^{72}_{31}\mathrm{Ga}^{*}_{\mathrm{isu}} \rightarrow {}^{72}_{32}\mathrm{Ge} + \mathrm{e}^{-} + \tilde{\nu} + \nu\tilde{\nu} + Q(9.74\ \mathrm{Mev}). \quad (33)$$

The analysis of these processes shows that, in accordance with the data in Table 6, all impurity zinc isotopes must participate with similar efficiencies in nuclear transformations initiated by interactions with neutral ${}^{1}\mathrm{n}_{\mathrm{isu}}$ nuclei.

The processes that determine the reduction in the content of stable iron isotopes in the nickel cathode, detected in the experiments, should be considered together with nuclear transformations involving stable monoisotopes: manganese-55 and cobalt-59 produced in these processes, since the detected content of these isotopes in the initial nickel cathode also dropped noticeably. After 40-hour treatment in a glow discharge, the manganese content in the near-surface region of the nickel sample dropped to 4% and the cobalt content to 34.6% of the initial one. Let us imagine a possible combination of such nuclear-chemical transformations making it possible to qualitatively understand the cause of the reduction in the initial content of all iron isotopes. We assume that the interaction of the Fe-54 nucleus with the Fe nucleus and the production of the compound Fe-55 nucleus in the isu-state initiates an interaction with the inner-shell electron (it is known that the Fe-55 nucleus in the ground state undergoes K-capture), leading to the production of the Mn-55 nucleus, which can be represented as a gross process

$$^{54}_{26}\mathrm{Fe} + {}^{1}\mathrm{n}_{\mathrm{isu}} \rightarrow {}^{55}_{26}\mathrm{Fe}^{*}_{\mathrm{isu}} \xrightarrow[\mathrm{e}^{-}]{} {}^{55}_{25}\mathrm{Mn} + \nu + \nu\tilde{\nu} + Q(8.75\ \mathrm{MeV}). \quad (34)$$

The Mn-55 nuclei produced in this case can also participate in nuclear transformations due to interaction with neutral ${}^{1}\mathrm{n}_{\mathrm{isu}}$ nuclei:

$$^{55}_{25}\mathrm{Mn} + {}^{1}\mathrm{n}_{\mathrm{isu}} \rightarrow {}^{56}_{25}\mathrm{Mn}^{*}_{\mathrm{isu}} \rightarrow {}^{56}_{26}\mathrm{Fe} + \mathrm{e}^{-} + \tilde{\nu} + \nu\tilde{\nu} + Q(10.18\ \mathrm{MeV}). \quad (35)$$

The other processes are represented as

$$^{56}_{26}\mathrm{Fe} + {}^{1}\mathrm{n}_{\mathrm{isu}} \rightarrow {}^{57}_{26}\mathrm{Fe}^{*}_{\mathrm{isu}} \rightarrow {}^{57}_{26}\mathrm{Fe} + \nu\tilde{\nu} + Q(6.86\ \mathrm{MeV}), \quad (36)$$

$$^{57}_{26}\mathrm{Fe} + {}^{1}\mathrm{n}_{\mathrm{isu}} \rightarrow {}^{58}_{26}\mathrm{Fe}^{*}_{\mathrm{isu}} \rightarrow {}^{58}_{26}\mathrm{Fe} + \nu\tilde{\nu} + Q(9.26\ \mathrm{MeV}), \quad (37)$$

$$^{58}_{26}\mathrm{Fe} + {}^{1}\mathrm{n}_{\mathrm{isu}} \rightarrow {}^{59}_{26}\mathrm{Fe}^{*}_{\mathrm{isu}} \rightarrow {}^{59}_{27}\mathrm{Co} + \mathrm{e}^{-} + \tilde{\nu} + \nu\tilde{\nu} + Q(7.36\ \mathrm{MeV}), \quad (38)$$

$$^{59}_{27}\mathrm{Co} + {}^{1}\mathrm{n}_{\mathrm{isu}} \rightarrow {}^{60}_{27}\mathrm{Co}^{*}_{\mathrm{isu}} \rightarrow {}^{60}_{28}\mathrm{Ni} + \mathrm{e}^{-} + \tilde{\nu} + Q(9.53\ \mathrm{MeV}). \quad (39)$$

It should be noted that the fraction of the Fe-58 isotope usually does not exceed 0.3% of the total iron content and is not detected under the conditions of our experiments in the analysis against the background of nickel-58. Therefore, it can be assumed that a noticeable amount of Co-59 against the background of the initially existing impurity in the nickel sample during the treatment of the nickel cathode, in accordance with (38), is not produced and process (39) should be associated with a reduction in the amount of impurity cobalt.

In connection with the introduction into consideration of the neutron-like particles ${}^{1}\mathrm{n}_{\mathrm{isu}}$, ${}^{2}\mathrm{n}_{\mathrm{isu}}$, and ${}^{3}\mathrm{n}_{\mathrm{isu}}$, making it possible to understand the physical reasons for the initiation of low-energy nuclear chemical processes, it is necessary to analyze more carefully the phenomenon of neutron production in various low-energy nuclear processes studied since the 1950s by Artsimovich's group [5, 6], in the works of Basov et al. [10], Deryagin et al. [17], in recent works by Schenkel et al. [19], work [20] considering laser impacts on deuterated titanium targets, and the work of a NASA scientific group using bubble detectors of neutrons, which is considered the most accurate method [21]. It cannot be ruled out that, in all these studies, in a deuteron-containing medium, β dineutrons were produced, which, in neutron detectors based on the neutrons absorption and the subsequent emission of charged particles or γ quanta, could initiate $\left({}^{2}\mathrm{n}_{\mathrm{isu}}, {}^{1}\mathrm{n}_{\mathrm{isu}}\right)$ processes in which a neutron is absorbed and a neutral ${}^{1}\mathrm{n}_{\mathrm{isu}}$ particle is emitted perceived as a neutron, although the mass of this particle is lower than the mass of a neutron by 0.78 MeV/c^2.

It is especially worth mentioning the work of Klimov et al. [22], in which, when creating pulsed discharges in a vortex plasma reactor, particles were detected defined in [22] as neutrons, but different from them and termed as neutron-like. These particles were detected as neutrons in gas proportional He-3 SPRS detectors only above certain threshold voltages (>3.6–4.2 kV) in the reactor discharge-chamber detectors. However, when such particles were detected with a KRAN-1 radiometer by the detected luminescence of a plastic scintillator, the shape of the optical signal was totally different from that when calibrating this device with neutrons. Moreover, according to [22], fluxes of neutron-like particles did not initiate artificial radioactivity in indium samples with the forma-

tion of metastable isomers of In-116 and In-114 with several half-lives, as is typical of neutrons [44, 45].

The totality of all this information gives ground to believe that it was the $^{1}n_{isu}$ particles that were fixed in the experiments of Klimov's group [22]. It should be noted that, since the mass of the neutral $^{1}n_{isu}$ nuclei we introduced is equal to the mass of the protium atom, the detection of such a particle as a neutron in proportional He-3 counters, which occurs upon the production of a proton and a tritium nucleus, turns out to be a threshold process with an energy $E_{th} = 19$ keV. However, considering the voltage applied to the discharge chamber of a vortex plasma reactor [22], which exceeds the above threshold values U_d^*, it can be assumed that, in nonequilibrium pulsed discharges, the kinetic energy of particles produced in process (4) will exceed this threshold. As for the negative result in the initiation of artificial radioactivity of indium by fluxes of neutron-like particles, the production of a compound In nucleus with a neutral $^{1}n_{isu}$ nucleus having a disturbed nucleon structure obviously complicates the necessary restructuring of the nuclear matter of the compound nucleus, the relaxation of which, as might be assumed, will be realized in a more natural way through emission of $\nu\tilde{\nu}$ pairs rather than γ quanta, as in the case of a well-defined nucleon structure of excited nuclei.

It is not excluded that the creation of $^{2}n_{isu}$ nuclei was detected earlier. We mean the work [46], in which the spectra of "lost mass" for the reaction $^{6}Li(\pi^{-},p)^{5}H$ were investigated (see also Fig. 1 in [33]). Naturally, the whole range of issues related to the detection of metastable neutral nuclei $^{1}n_{isu}$ and $^{2}n_{isu}$ requires further experimental study.

5. CONCLUDING REMARKS

Let us emphasize two aspects of this work, which made it possible to realize low-energy nuclear-chemical processes of artificial radioactivity with the conversion of nonradioactive impurity elements in metal cathodes into radioactive ones under the conditions of a hydrogen-containing glow-discharge plasma and, using the ICP MS technique, to understand the causes of the high efficiency of the effects on cathodes of plasma flows, the characteristic energy density of which is 5–6 orders of magnitude lower than those usually used in nuclear physics experiments.

(1) Finding the modes of generation of current pulses that are abnormally high for a glow discharge, regularly manifested locally on the cathode work surface and stochastically changing their localization, the unsteady current structure of which turns out to be highly specific for different cathode materials.

(2) Introduction of the concept of the existence in nuclear matter of nonnucleon metastable excitations initiated by electrons of high (in terms of chemical scales) energies and sufficiently long-lived, which determines the existence of light neutral nuclei: β neutron $^{1}n_{isu}$ and β dineutron $^{2}n_{isu}$, which, in the absence of Coulomb barriers, effectively participate in nuclear-chemical processes, forming compound nuclei with target nuclei. It should be emphasized that the masses of these nuclei, equal to the masses of protium and deuterium atoms, respectively, as well as the decisive role of weak interactions in structural rearrangements and the removal of excitation of the emerging compound nuclei by the URCA process: emission of neutrino–antineutrino pairs, determine the safety of the manifestation of these particles in nuclear processes [33, 34, 37].

CONFLICT OF INTEREST

The authors declare that they have no conflicts of interest.

REFERENCES

1. M. Fleishmann, S. Pons, and M. Hawkins, "Electrochemical induced nuclear fusion of deuterium," J. Electroanal. Chem. **261**, 301–308 (1989).
2. G. L. Wendt and C. E. Irion, "Experimental attempts to decompose tungsten at high temperatures," J. Am. Chem. Soc. **44**, 1887–1894 (1922).
3. E. Rutherford, "Disintegration of elements," Nature-London **109**, 418 (1922).
4. G. L. Wendt, "Decomposition of tungsten," Science, New Series **55** (1430), 567 (1922).
5. L. A. Artsimovich, E. I. Dobrokhotov, S. Yu. Luk'yanov, et al., "Neutron radiation from a gas discharge," At. Energ. **3**, 84–87 (1956).
6. I. V. Kurchatov, "On the possibility of creation of thermonuclear reactions in a gas discharge," Usp. Fiz. Nauk **59**, 603–618 (1956).
7. B. A. Trubnikov, *Plasma Theory* (Energoatomizdat, Moscow, 1996).
8. V. V. Vikhrev and V. D. Korolev, "Generation of neutrons in Z-pinches," Plasma Phys. Rep. **33**, 356–380 (2007).
9. Yu. V. Matveev, "Plasma dynamics and generation of hard radiations in experiments with cylindrical Z-pinches," Plasma Phys. Rep. **36**, 200–215 (2010).
10. N. G. Basov, S. D. Zakharov, P. G. Kryukov, Yu. V. Senatskii, and S. V. Chekalin, "Experiments on observation of neutrons upon focusing of a powerful laser radiation on a lithium deuteride surface," Preprint FIAN No. 63 (Lebedev Physical Institute, Moscow, 1968); Pis'ma Zh. Eksp. Teor. Fiz. **8**, 26 (1968).
11. V. I. Vysotskii, A. A. Kornilova, and M. V. Vysotskyy, "Features and mechanisms of generation of neutrons and other particles in first laser fusion experiments," JETP **131**, 566–571 (2020).
12. S. Fritzler, Z. Najmudin, V. Malka, et al., "Ion heating and thermonuclear neutron production from high-intensity subpicosecond laser pulses interacting with underdense plasmas," Phys. Rev. Lett. **89**, 165004 (2002).

13. C. Labaune, C. Baccou, S. Depierreux, et al., "Fusion reactions initiated by laser-accelerated particle beams in a laser-produced plasma," Nat. Commun. **4**, 2506 (2013); arXiv:1310.2002v1.
14. G. V. Karasev, N. A. Krotova, and B. V. Deryagin, "Study of a gas discharge upon detachment of high-polymer film from a solid substrate," Dokl. Akad. Nauk SSSR **89**, 109–112 (1953).
15. G. A. Sokolina, N. A. Krotova, and Yu. A. Khrustalev, "Study of properties of a polymer–semiconductor interface," Dokl. Akad. Nauk SSSR **147**, 1409–1412 (1962).
16. B. V. Derjaguin, V. A. Klyuev, A. G. Lipson, and Yu. P. Toporov, "Possibility of nuclear reactions during the fracture of solids," Colloid Journ. USSR **48**, 8–10 (1986).
17. B. V. Derjaguin, V. A. Kluev, A. G. Lipson, and Yu. P. Toporov, "Excitation of nuclear reaction under mechanical effect (impact) on deuterated solids," Physica B **167**, 189–193 (1990).
18. T. Schenkel, A. Persaud, H. Wang, et al., "Investigation of light ion fusion reactions with plasma discharges," J. Appl. Phys. **126**, 203302 (2019).
19. V. Pines, M. Pines, A. Chait, et al., "Nuclear fusion reactions in deuterated metals," Phys. Rev. C **101**, 044609 (2020).
20. D. M. Golishnikov, V. M. Gordienko, N. V. Eremin, et al., "Laser-induced deuteration of a titanium target and neutron generation under the action of superintense femtosecond laser radiation," Laser Phys. **15**, 1154–1162 (2005).
21. P. J. Smith, R. C. Hendricks, and B. M. Steinetz, "Electrolytic co-deposition neutron production measured by bubble detectors," J. Electroanal. Chem. **882**, 115024 (2021).
22. A. I. Klimov, N. K. Belov, and B. N. Tolkunov, "Neutron flux and soft X-radiation created by heterogeneous plasmoid," J. Phys. Conf. Ser. **1698**, 012034 (2020).
23. *Proceedings of the ICCF 22 Conference, Sept. 8–13, 2019, Assisi, Italy*; J. Condens. Matter Nucl. Sci. **33**, 1–339 (2020).
24. *The 21st Meeting of Japan CF Research Society. JCF21 Abstracts, Dec. 11-12, 2020*: http://lenr.seplm.ru/konferentsii/tezisy-dokladov-21-vstrechi-yaponskogo-obshchestva-po-kholodnomu-sintezu-11-12-dekabrya-2020.
25. I. B. Savvatimova, Ya. Kucherov, and A. B. Karabut, "Cathode material change after deuterium glow discharge," Trans. Fusion Techn. **26**, 389–394 (1994).
26. I. B. Savvatimova, "Transmutation of elements in low-energy glow discharge and the associated processes," J. Cond. Matter Nucl. Sci. **6**, 181–198 (2012); www.isccmns.org/CMNS/JCMNS-Vol6.pdf.
27. A. B. Karabut, Ya. R. Kucherov, and I. B. Savvatimova, "Nuclear product ratio for glow discharge in deuterium," Phys. Lett. A **170**, 265–272 (1992); www.lenr-canr.org/acrobat/KarabutABnuclearpro.pdf.
28. E. V. Barmina, I. A. Sukhov, N. M. Lepekhin, et al., "Application of copper vapor lasers in control of activity of Uranium isotopes," Quant. Electron. **43**, 591–596 (2013).
29. G. A. Shafeev, F. Bozon-Verduraz, and M. Robert, "Experimental evidence of transmutation of Hg into Au under laser exposure of Hg nanodrops in D_2O," Phys. Wave Phenom. **15** (3), 131–136 (2007).
30. A. V. Simakin and G. A. Shafeev, "Initiation of nuclear reactions under laser irradiation of metal nanoparticles in the presence of thorium aqua ions," Phys. Wave Phenom. **16**, 268–274 (2008).
31. E. V. Barmina, S. F. Timashev, and G. A. Shafeev, "Laser-induced synthesis and decay of tritium under exposure of solid targets in heavy water," J. Phys. Conf. Ser. **688**, 012106 (2016); http://arxiv.org/abs/1306.0830 [physics.gen-ph].
32. S. N. Andreev and G. A. Shafeev, "Nonlinear quenching of radioactivity of aqueous solutions of salts of nucleons upon laser ablation of metal nanoparticles," RENSIT **9**, 65–73 (2017).
33. S. Timashev, "On mechanisms of low-energy nuclear-chemical processes," RENSIT **9**, 37-51 (2017); http://rensit.ru/vypuski/article/200/9(1)37-51.pdf.
34. S. Timashev, "Metastable nonnucleonic states of nuclear matter: phenomenology," Int. J. Phys. Sci. **15** (2), 1–25 (2017); http://www.sciencedomain.org/issue/2727.
35. S. F. Timashev, A. V. Simakin, and A. G. Shafeev, "Nuclear-chemical processes under the conditions of laser ablation of metals in aqueous media (problems of "cold fusion")," Russ. J. Phys. Chem. A **88**, 1980–1988 (2014).
36. S. F. Timashev, "Radioactive decay as a forced nuclear chemical process: Phenomenology," Russ. J. Phys. Chem. A **89**, 2072–2083 (2015).
37. S. F. Timashev, "Physical vacuum as a system manifesting itself on various scales – from nuclear physics to cosmology," arXiv:1107.1799v8 [physics.gen-ph].
38. I. B. Savvatimova and A. B. Karabut, "Products of nuclear reactions detected on the cathode after glow discharge experiments in deuterium," Poverkhnost', **1**, 63–75 (1996).
39. S. A. Thomas, F. D. Abdalla, and O. Lahav, "Upper bound of 0.28 eV on neutrino masses from the largest photometric redshift survey," Phys. Rev. Lett. **105**, 031301 (2010).
40. S. Timashev, "Nuclear-chemical processes in the solar atmosphere," Int. J. Astrophys. Space Sci. **2** (6), 88–92 (2014).
41. J. M. Lattimer, C. J. Pethick, M. Prakash, and P. Haensel, "Direct URCA process in neutron stars," Phys. Rev. Lett. **66**, 2701–2704 (1991).
42. N. N. Tunitskii, V. A. Kaminskii, and S. F. Timashev, *Methods of Physico-Chemical Kinetics* (Khimiya, Moscow, 1972) [in Russian].
43. M. Albertsson, B. G. Carlsson, T. Dossing, et al., "Correlation studies of fission-fragment neutron multiplicities," Phys. Rev. C **103**, 014609 (2021).
44. L. I. Rusinov, "Nuclear isomerism," Sov. Phys. Usp. **73**, 282–290 (1961).
45. I. I. Gurevich and V. P. Protasov, *Neutron Physics* (Energoatomizdat, Moscow, 1997)
46. K. K. Seth, and B. Parker, "Evidence for dineutrons in extremely neutron-rich nuclei," Phys. Rev. Lett. **66**, 2448–2451 (1991).

Translated by E. Chernokozhin